PERGAMON

Planetary and Space Science 49 (2001) 1211–1218

Planetary and Space Science

www.elsevier.com/locate/planspasci

Lyapunov exponent and entropy of the solar wind flow

Stefano Redaelli *, Wiesław M. Macek

Space Research Centre, Polish Academy of Sciences, Bartycka 18A, 00-716 Warsaw, Poland

Received 7 August 2000; received in revised form 29 September 2000; accepted 9 October 2000

Abstract

We analyse time series of velocity fluctuations of the low-speed stream of the solar wind measured by the Helios spacecraft in the inner heliosphere. We use a nonlinear filter to give faithful representation of nonlinear behaviour of the flow. We demonstrate that the influence of noise in the data records can be much more efficiently reduced by a nonlinear filter than with conventional filters. We argue that due to this nonlinear noise reduction we get with much reliability estimates of the largest Lyapunov exponent and the Kolmogorov entropy. The Lyapunov exponent and the entropy are plausibly positive, which would exhibit sensitivity to initial conditions. These results show that the solar wind in the inner heliosphere is likely a deterministic *chaotic* system. We hope that these studies could shed light on the physical mechanism of coronal structure.

PACS: 05.45.Tp; 96.50.Ci; 95.10.Fh

Keywords: Nonlinear time series analysis; Solar wind plasma; Lyapunov exponents; Entropy

1. Introduction

The entropies and the Lyapunov exponents are very important characteristics of complex dynamical systems. The Kolmogorov entropy is the rate of creation of information as a chaotic orbit evolves (Schuster, 1989; Ott, 1993; Ott et al., 1994). The entropy is equal to zero for a regular (periodic) system, a constant greater than zero for a *chaotic* deterministic system, and infinite for a stochastic random system; a positive and finite entropy implies chaos. The chaotic attractor has at least one unstable direction corresponding to a positive Lyapunov exponent. Basically, chaos arises from the exponential growth of infinitesimal perturbations, together with global folding mechanisms to guarantee boundedness of the trajectories describing the system in phase space. The properly averaged exponent of this increase is characteristic for the system underlying the data and quantifies chaos and is called the Lyapunov exponent (Schuster, 1989; Ott, 1993; Ott et al., 1994). However, both the Lyapunov exponent and entropy describe a kind of scaling behaviour in the limit as the distances r between points on the attractor approach zero. These characteristics are sensitive to the presence of small amounts of noise, which may obscure the underlying scaling properties, unless the data are filtered to reduce noise contamination. In particular, a zero entropy or Lyapunov exponent can be driven positive by noise, or in the latter case just drift slightly positive as the exponent fluctuates near zero. Therefore, in order to detect and quantify chaos in any real dynamical system, it is necessary to deal with a cleaned experimental signal.

Following space physics applications, e.g., Kurths and Herzel (1987), Carbone et al. (1995), we consider the inner heliosphere. Since the 1960s we have known that besides electromagnetic radiation, the Sun also radiates charged particles forming a plasma blowing nearly radially outward from the Sun. The solar wind plasma flowing supersonically away from the Sun is quite well modelled within the framework of hydromagnetic theory. This continuous flow has two forms: slow (≈ 300 km s^{-1}) and fast (≈ 900 km s^{-1}) (Schwenn, 1990). The fast wind is associated with coronal holes and is relatively uniform and stable, while the slow wind is quite variable in terms of velocities. Indication for a chaotic attractor in the slow solar wind has recently been given in Macek (1998, 1999), Macek and Obojska (1996, 1997, 1998). In particular, Macek (1998) has provided tests for nonlinearity in the solar wind data, including a powerful method of singular-value decomposition (Albano et al., 1988) and statistical surrogate data tests (Theiler et al., 1992). Further, Macek and Redaelli (2000) have shown that the Kolmogorov entropy of the attractor is positive and finite, as it holds for a *chaotic* system.

In this paper, we have extended our previous results on dimensional time series analysis (Macek, 1998) and

* Corresponding author. Fax: +4822-840-3131.
E-mail address: redaelli@cbk.waw.pl (S. Redaelli).

0032-0633/01/$ - see front matter
PII: S0032-0633(01)00062-9

estimating of the Kolmogorov entropy (Macek and Redaelli, 2000). Namely, we focus on the maximal Lyapunov exponent of the solar wind that should be consistent with the Kolmogorov entropy. Therefore, we apply the modern technique of nonlinear noise reduction (Schreiber, 1993a, b; Kantz et al., 1993), which allows a more realistic calculation of these characteristics of the solar wind flow, directly from the cleaned experimental signal. The data and importance of noise reduction are discussed in Section 2. The method of estimation of the entropy and Lyapunov exponent is reviewed in Section 3. Section 4 is devoted to the main results of our calculations. In particular, we show that the correlation entropy and the largest Lyapunov exponent are positive and finite, as it should be for a *chaotic* system. The dimension is only briefly discussed in Section 4. In this way, we have further supported our previous conjecture that trajectories describing the system in the inertial manifold of phase space asymptotically approach the attractor of low-dimension. These results provide some evidence that the complex low-speed solar wind is likely a deterministic *chaotic* system. One can also expect that this attractor should contain information about the dynamic variations of the coronal streamers. It is also possible that it represents a structure of the time sequence of near-Sun coronal fine-stream tubes, see Macek (1998), Macek and Redaelli (2000) and references therein. Naturally, fast-speed streams should have quite different dynamics, and we have not yet found any scaling properties similar to those for the slow wind. We limit our study to the low-speed stream.

2. Data and noise

We analyse the Helios data using the radial velocity component v, measured in the heliosphere at $\sim$ 0.3 AU (Schwenn, 1990). These raw data of $N = 4514$ points, with sampling time of $\Delta t = 40.5$ s, are presented in Fig. 1(a). As discussed in Macek (1998), slow trends $(349.7 + 21.74t - 96.61t^2$, with t being a fraction of the total sample) were subtracted from the raw data and the resulting original data after detrending are now denoted by $x_i = v(t_i)$, in km s^{-1}, $i = 1, \ldots, N$. The chosen interval is (after detrending) typical for the low-speed solar wind during roughly stationary conditions, i.e., if nothing dramatic happens (with no shocks, discontinuities, etc.). The samples near the Sun and near the Earth's orbit (during the solar minimum and maximum) give basically the same main results; may be the solar wind fluctuations are more turbulent near the Sun. Therefore, we have chosen a sample near the Sun. Anyway, the same sample is chosen by Macek (1998), Macek and Redaelli (2000), and in the present paper in order to compare three important characteristics of the solar wind flow, namely: dimension, entropy, and Lyapunov exponent, correspondingly.

However, in Macek (1998, Fig. 1(b)) these data were eightfold smoothed (replacing each data point with the average of itself and its two nearest neighbours). Certainly, this is a particular linear final impulse response (FIR) filter, which should preserve the correlation dimension (Ott et al., 1994). On the other hand, in order to use filters correctly and to check their efficiency, it is important to estimate the level of noise in the data before and after filtering (cf. Badii et al., 1988). Therefore, we have discussed the influence of noise reduction in detail in Macek and Redaelli (2000).

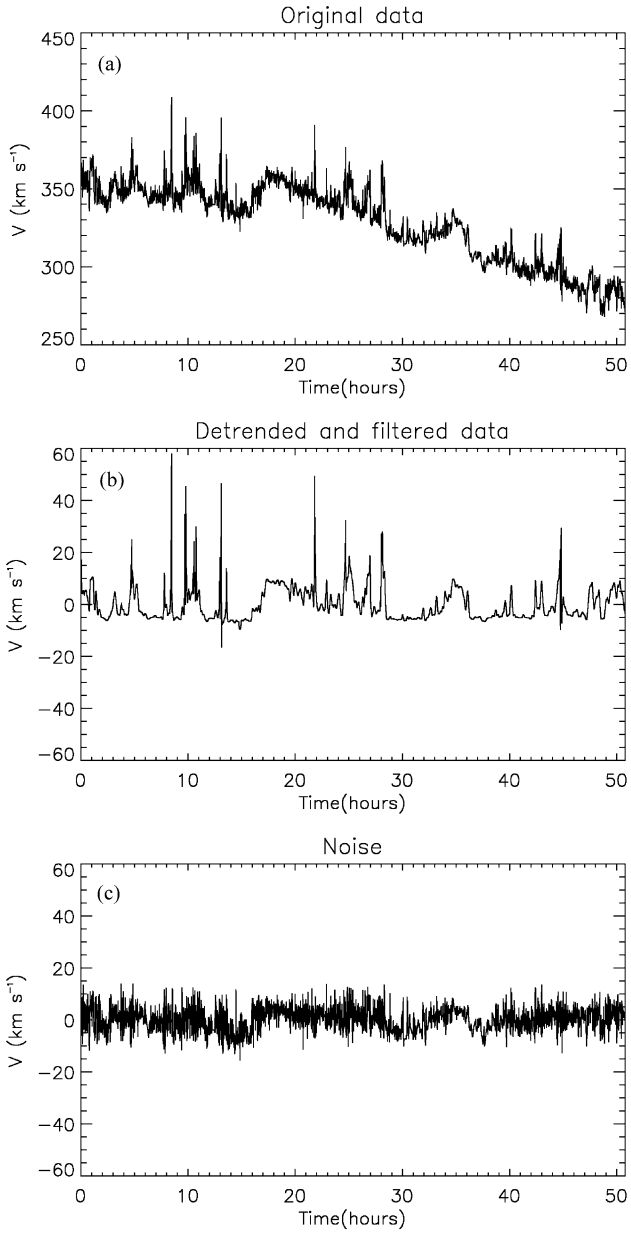

Fig. 1. The radial velocity v observed by the Helios 1 spacecraft in 1975 from 67:08:20.5 to 69:11:07 (day:h:min) at distances 0.32 AU from the Sun; (a) the original data, (b) the detrended filtered data after nonlinear noise reduction, and (c) the noise removed by nonlinear filter.

More specifically, following Schreiber and Kantz (1995), our approach to noise reduction is to assume that the unknown true signal y_i is generated by a deterministic

dynamics, whereas the noise η_i is random, i.e., one measures the noisy signal $x_i = y_i + \eta_i$. This is often referred as measurements noise, which does not need necessarily be 'instrumental' only. Often the noise enters the dynamics in a more subtle way (dynamical noise, rather than measurement noise), and the two cannot be disentangled even in principle. In general, we do not know a priori, which kind of noise we have in the data, except may be instrumental errors. Admittedly, this puts any interpretation of the data on shaky ground. However, we believe that in our case there are underlying dynamical processes upon which the noise has been superimposed, see Macek (1998), Macek and Redaelli (2000). Here, as in Macek and Redaelli (2000), we assume that the data can be decomposed into two components. $x_i = y_i + \eta_i$, the clean signal and some additive noise. The idea is to replace the measurement x_i, which contains noise, by a 'cleaned' value $x_i^c \approx y_i$. For example, in the case of the moving average FIR filter we would have

$$x_i^c = \frac{1}{2l+1} \sum_{j=-l}^{l} x_{i+j}. \tag{1}$$

The estimated noise level in the original data is 4–6% (Macek, 1998; Macek and Redaelli, 2000). Certainly, the moving average filter removes some amount of noise. However, we have verified that after the moving average linear filter of Eq. (1) we still have a substantial amount of noise of 2–5%, preventing us from any reliable estimation of the entropy and Lyapunov exponent.

Instead of using this linear filtering of the signal, we apply a nonlinear filter in order to reduce the noise more efficiently and to give a faithful representation of the nonlinear behaviour of the solar wind. Many sophisticated nonlinear filtering algorithms are available that exploit the local dynamical behaviour to identify and remove noise from the experimental data, for a review see, e.g., Kostelich and Schreiber (1993). For example, projective schemes move the observations at each point onto a subspace that approximates the tangent plane to the manifold containing the attractor in the phase space of the system (Kantz et al., 1993). These algorithms imply global or local approximation of the underlying dynamics inferred from the data. One of these nonlinear filters proposed by Schreiber is very simple; we just replace each point on the noisy trajectory by the average value of its neighbours (Schreiber, 1993a). In some way, this average could be regarded as a 'zero-order' approximation of this dynamics locally by a constant. Surprisingly, this extremely simple nonlinear filter is very efficient, especially for short and slightly noisy data. The advantages of this particular method are also discussed by Macek and Redaelli (2000). We have shown that in the case of the solar wind data the noise has been reduced by half an order of magnitude, below 1%. Therefore, as in Macek and Redaelli (2000), in this paper we use the Schreiber filter.

More specifically, the nonlinear Schreiber filter works in embedding space of dimension $2l + 1$ (Schreiber, 1993a). We construct vectors in this embedding space that involve past and future coordinates $\mathbf{X}_i = (x_{i-l}, \ldots, x_{i+l})$, define a neighbourhood of size ε, $|\mathbf{X}_i - \mathbf{X}_j| < \varepsilon$, and then replace the data point x_i by its mean value in the neighbourhood,

$$x_i^c = \frac{1}{n_i} \sum_{|\mathbf{X}_i - \mathbf{X}_j| < \varepsilon} x_j, \tag{2}$$

where n_i is the number of elements of this neighbourhood Schreiber (1993a).

In practice, we average over segments of the trajectory that are close for l time steps in the past and l in the future. The size of the neighbourhood should be larger than the noise level assumed in the data. The procedure can be iterated taking decreasing ε until no neighbours are found and no further correction is made (usually 2–3 iterations are enough). Summarizing, we use the Schreiber filter, which averages in embedding space of a chosen dimension $2l + 1$ and a defined neighbourhood of size ε, about 2–3 times of the estimated initial noise level (Schreiber, 1993a). We have performed three iterations taking the following input parameters: $l = 3$, $\varepsilon = 0.15$; $l = 6$, $\varepsilon = 0.08$; and $l = 6$, $\varepsilon = 0.012$. The filtered data after this procedure are shown in Fig. 1(b), and the noise (that is the difference between the original data in Fig. 1(a) after detrending and the filtered data) is presented in Fig. 1(c). It is worth noting that only after nonlinear filtering has the noise efficiently been reduced to 0.3–0.9% i.e., by half an order of magnitude, as compared with the original data.

Using our time series of equally spaced, detrended and cleaned data, x^c, we construct a large number of vectors in the embedding phase space of dimension m, $\mathbf{X}(t_i) = [x^c(t_i), x^c(t_i + \tau), \ldots, x^c(t_i + (m-1)\tau)]$, where $i = 1, \ldots, n$ with $n = N - (m-1)\tau$. Obviously, the elements of vectors are not really independent, even before filtering. However, before calculating a particular characteristic of the attractor, we choose a proper delay time, τ, for the vectors constructed from the cleaned experimental data, i.e., after detrending and nonlinear noise reduction as discussed in Macek (1998). This make certain that elements of each vectors after nonlinear noise reduction are at least linearly time independent. Therefore, we hope that this does not affect the correlation entropy and the maximal Lyapunov exponent.

As in Macek (1998), Macek and Redaelli (2000), we choose for the entropy a time delay $\tau = 250\Delta t$ slightly larger than the first zero of the autocorrelation function, $t_0 = 212\Delta t$, $(\langle x^c(t) x^c(t + t_0)\rangle - \langle x^c(t)\rangle^2)/\sigma^2 = 0$ with average velocity $\langle x^c\rangle = 0.02$ km s^{-1} and standard deviation $\sigma = 8.07$ km s^{-1}. Table 1 summarizes selected calculated characteristics of the detrended data cleaned by using of the Schreiber filter shown in Fig. 1(b); note also t_a in Table 1 when the autocorrelation function decreases by a factor of $1/e$.

Table 1
The solar wind velocity fluctuations data after nonlinear noise reduction

Number of data points, N	4514
Sampling time, Δt	40.5 s
Skewness, κ_3	1.88
Kurtosis, κ_4	7.53
Autocorrelation time, t_a	1.6×10^3 s
Correlation dimension[a], D_2	2.7 ± 0.3
Entropy[b] ($q=2$), K_2	0.10 ± 0.06
Largest Lyapunov exponent[c], λ_{max}	0.10 ± 0.02
Predictability horizon time	$\sim 10^4$ s

[a]The average slope for $6 \leqslant m \leqslant 10$ is taken as D_2.
[b]The average ($\Delta m = 3$) spacing between slopes for $8 \leqslant m \leqslant 12$ is taken as K_2.
[c]In the same units as K_2 (base e).

3. Entropy and Lyapunov exponent

The conventional Boltzmann entropy (zero order, $q=0$) gives information about the number of states available for the dynamical system in phase space (for a given precision r, it is the number of boxes of size r). Therefore, it does not provide any information how the system evolves; this measure of disorder is, therefore, useful only for stochastic systems (conventional thermodynamics, assuming that the system is at equilibrium and all accessible microscopic states are visited equally). Instead, we use here the Renyi–Kolmogorov generalized q-order entropy that takes into account how often these states are visited by a trajectory, i.e., provides information about the evolution of the system. Thereby, in particular, the Kolmogorov–Sinai information entropy ($q=1$) and the correlation entropy ($q=2$) provide important information about the dynamics and are useful also for nonlinear deterministic systems (the latter is easier to calculate). It is worth noting, in particular, that the system that creates information as its orbit evolves is certainly chaotic. On the other hand, stochastic noisy system occupies all available phase space, and in the ideal case (infinite number of states) the correlation entropy would be infinite.

The formal definition of the generalized entropy is as follows. We divide the embedding space into a large number $M(r)$ of equal hypercubes of size r, which cover the presumed attractor. If p_j is the probability measure that a point from a time series falls in a typical jth hypercube, using the q-order function $I_q(r) = \sum (p_j)^q$, $j = 1, \ldots, M$, the q-order Renyi information *entropy* measure is, e.g., Ott (1993), Ott et al. (1994), Grassberger and Procaccia (1983a),

$$K_q = \lim_{r\to 0} \lim_{m\to\infty} \frac{1}{1-q} \ln I_q(r). \tag{3}$$

The related generalized dimension given by $D_q = \lim_{r\to 0} [\ln I_q(r)/\ln r]/(q-1)$, see Ott (1993), Ott et al. (1994), has been discussed extensively in Macek (1998).

In practice, $q=2$ is sufficient and $I_2(r)$ is taken to be equal to the correlation sum (Grassberger and Procaccia, 1983b)

$$C_m(r) = \frac{1}{n_{ref}} \sum_{i=1}^{n_{ref}} \frac{1}{n - 2n_c - 1} \sum_{j=n_c+1}^{n} \theta(r - |\mathbf{X}(t_i) - \mathbf{X}(t_j)|) \tag{4}$$

with $\theta(x)$ being the unit step function, where $n_{ref} = 500$ is the number of reference vectors and $n_c = 4$ is Theiler's correction (Theiler, 1986). Since the correlation sum is simply an arithmetic average over the numbers of neighbours, this can yield meaningful results for the dimension and entropy even when the number of neighbours available for some reference points is limited in most real dynamical systems. For large m and small r it can be argued that

$$C_m(r) \propto r^{D_2} e^{-m K_2}, \tag{5}$$

where D_2 and K_2 are approximations of the ideal $r \to 0$ and $m \to \infty$ limits in Eq. (3) for $q=2$ (Grassberger and Procaccia, 1983a). Namely, for values of r inside the plateau in the dimensions plots, the factor r^{D_2} in Eq. (5) is almost constant, and we can determine the correlation entropy (second order, $q=2$) K_2, with the Grassberger and Procaccia method (Grassberger and Procaccia, 1983a), by plotting

$$K_{2,m}(r) = \frac{1}{\Delta m} \ln \frac{C_m(r)}{C_{m+\Delta m}(r)} \tag{6}$$

both versus r for various m, and versus m for various r. For sufficiently large m, and r in the scaling region, this should converge towards a constant K_2.

In general, the entropy K_q is at most the sum of the positive Lyapunov exponents $\sum \lambda_k$, e.g., Ott et al. (1994). In particular, the correlation entropy K_2 should be its lower bound: $K_2 \leqslant \sum \lambda_k$ (positive). We restrict our calculations to the maximal Lyapunov exponent λ_{max}, which gives the averaged divergence rate of two initially closed trajectories, $\Delta_0 = |\mathbf{X}_i(0) - \mathbf{X}_j(0)|$, in the phase space

$$\Delta_t \approx \Delta_0 e^{\lambda_{max} t}, \tag{7}$$

where $\Delta_t = |\mathbf{X}_i(t) - \mathbf{X}_j(t)|$ is the distance between two vectors at time t.

Since we do not know the underlying equations of motion in the phase space of the system, we can try to estimate the maximal Lyapunov exponent λ_{max} directly from the time series. The first algorithm for this purpose has been proposed by Wolf et al. (1985). Unfortunately, it is not very robust and one can easily obtain wrong results, in particular in the presence of noise. It seems that this algorithm does not allow to test for the presence of exponential divergence, but just assume its existence and thus yields a finite exponent for stochastic data also, where the true exponent is infinite. Here, we use a quite robust algorithm of Kantz (1994), which tests directly for the exponential divergence of nearby trajectories. For each point of the reference trajectory several neighbouring trajectories are taken into consideration, averaging along the whole time series (not only

one trajectory as is in the Wolf et al.'s algorithm). Therefore, this method allows a much improved estimate of the largest Lyapunov exponent, even for small data set.

Namely, we construct reference vectors $\mathbf{X}_i$ in the embedding space of dimension m, using a time delay $\tau = 14\Delta t$ when the normalized autocorrelation function decreases to $1 - 1/e$. Then we search for all neighbours $\mathbf{X}_j$ in a neighbourhood of size ε, $|\mathbf{X}_i - \mathbf{X}_j| < \varepsilon$, and compute the average of the distances between all the neighbouring vectors and the reference vector, $\Delta_t = |x_{i+t} - x_{j+t}|$, as a function of t, i.e., the modulus of the difference of the tth scalar components of the two trajectories. The logarithm of the average distance is some effective expansion rate over the time span t. Then we average again over a large number of reference vectors along the whole trajectory ($N = 4000$ is taken). Therefore, we compute the function

$$S(t; m, \varepsilon) = \frac{1}{N} \sum_{i=1}^{n} \ln \left(\frac{1}{n_i} \sum_{|\mathbf{X}_i - \mathbf{X}_j| < \varepsilon} \Delta_t \right), \tag{8}$$

where n_i is the number of elements of this neighbourhood (Kantz and Schreiber, 1997).

If $S(t; m, \varepsilon)$ exhibits a linear increase with identical slope for all m larger than some m_0 and for a reasonable range of ε, than this slope is an estimate of $\lambda_{\max}$. In practice we have to choose two following parameters: m_0 which is usually equal to the correlation dimension, and ε which should be as small as possible to avoid saturation effects, but large enough such that on average each reference point has at least a few neighbours. Naturally, the size of the neighbourhood should be larger than the noise level assumed in the data.

4. Results and discussion

In Figs. 2–5 we show the results of our calculations as obtained for the following data sets: (a) the original data after detrending; (b) the cleaned experimental signal after nonlinear noise reduction; and (c) the noise that has been removed by the nonlinear filter, corresponding to Fig. 1(a)–(c), respectively.

In Fig. 2 we show the calculated probability distributions. The probability distribution for the cleaned data is non-Gaussian, Fig. 2(b), more clearly than for the moving average filter (cf. Macek, 1998). We have a large skewness of 1.88 (as compared with its normal standard deviation of 0.06) and a very large kurtosis of 7.53, see Table 1; the latter was small for the moving average filter. The calculated probability distribution of noise shown in Fig. 1(c) is roughly consistent with a normally distributed set of random numbers with $\sigma = 0.05$, see Fig. 2(c). In this way, we have verified that by use of the nonlinear Schreiber filter we have actually removed about 5% of the noise, leaving only a small non-Gaussian component (below 1%).

First, the vertical spacing between the straight lines $K_{2,\mathrm{m}}(r)$ of Eq. (6) calculated using the nonlinear filter

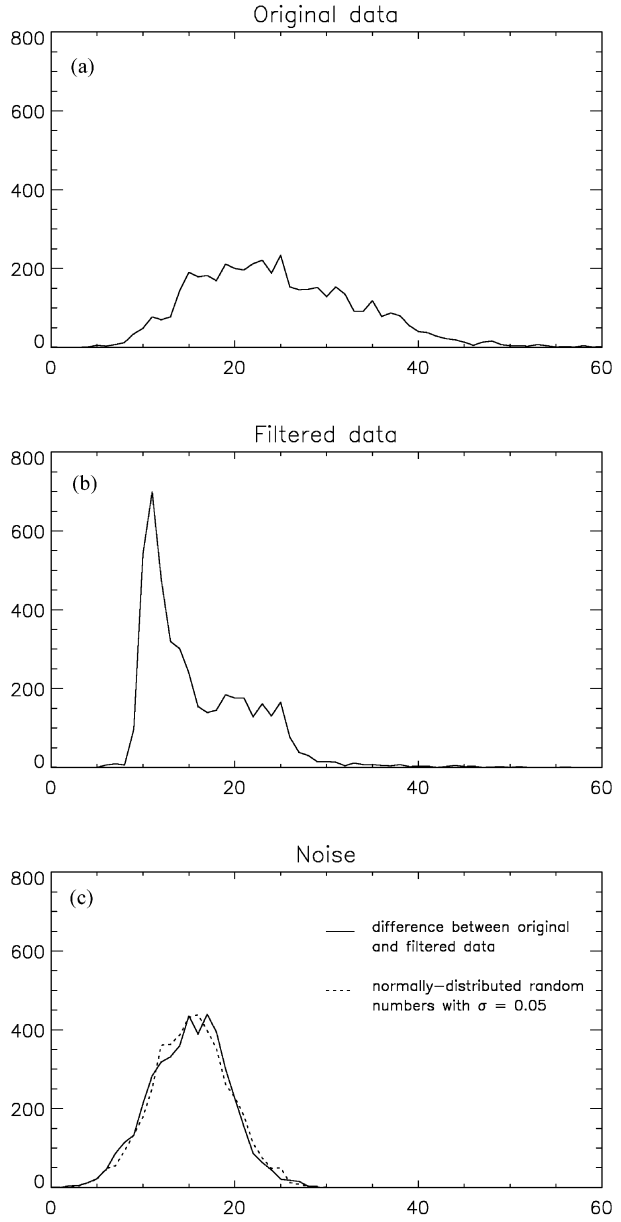

Fig. 2. The probability distribution functions as obtained for the following data sets: (a) the original data after detrending, (b) the filtered data after nonlinear noise reduction, and (c) the noise removed by nonlinear filter. The distribution of the difference between the original and filtered data (solid line) is consistent with a normally distributed set of random numbers with $\sigma = 0.05$ (dotted line).

versus the embedding dimension m (for $m = 4, \ldots, 12$) averaged over various distances r in the scaling region with a plateau is shown in Fig. 3, as discussed in Macek and Redaelli (2000). Again, only for the filtered data in Fig. 3(b) we see a clear saturation, while for the case of noise, Fig. 3(c), the calculated entropy increases with m, as it should be for a stochastic system. This demonstrates that the modern technique of nonlinear noise reduction (Schreiber, 1993a, b; Kantz and Schreiber, 1997) is necessary for a realistic calculation of the Kolmogorov entropy

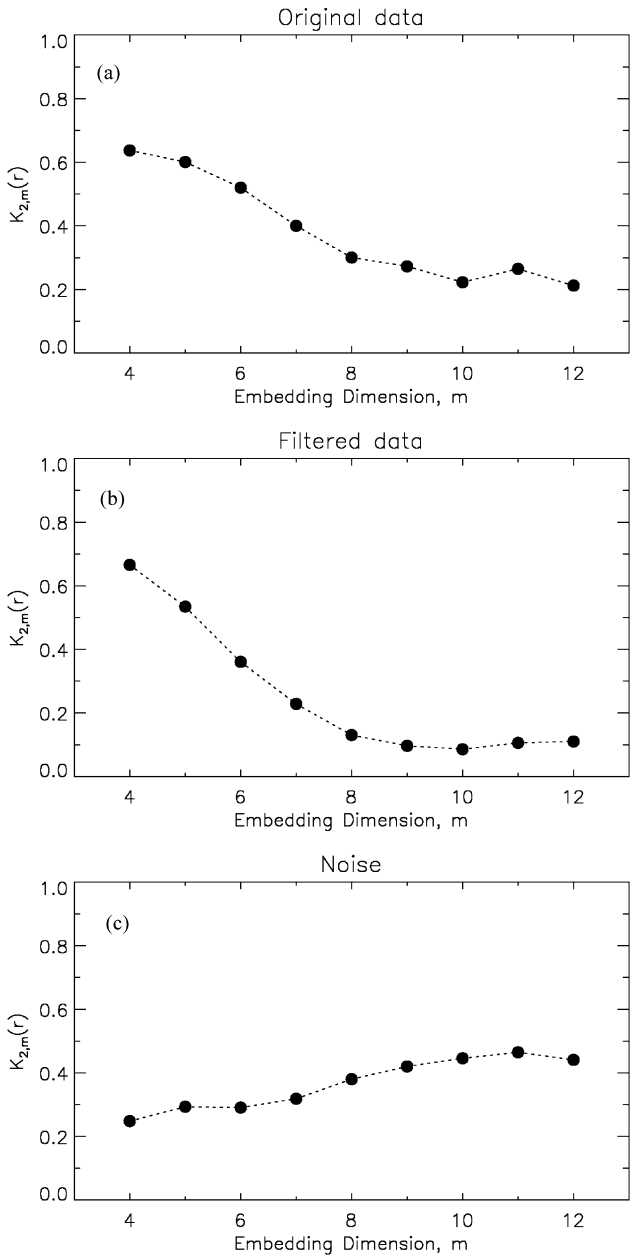

Fig. 3. The function $K_{2,m}(r)$ (base e) versus the embedding dimension m averaged over various distances r in the scaling region calculated for (a) original data after detrending, (b) cleaned experimental signal after nonlinear noise reduction, and (c) noise removed by nonlinear filter. Only in case (b) does the average saturated value yield the correlation entropy of $K_2 = 0.10 \pm 0.06$; see Tables 1 and 2, cf. Macek and Redaelli (2000, Fig. 3).

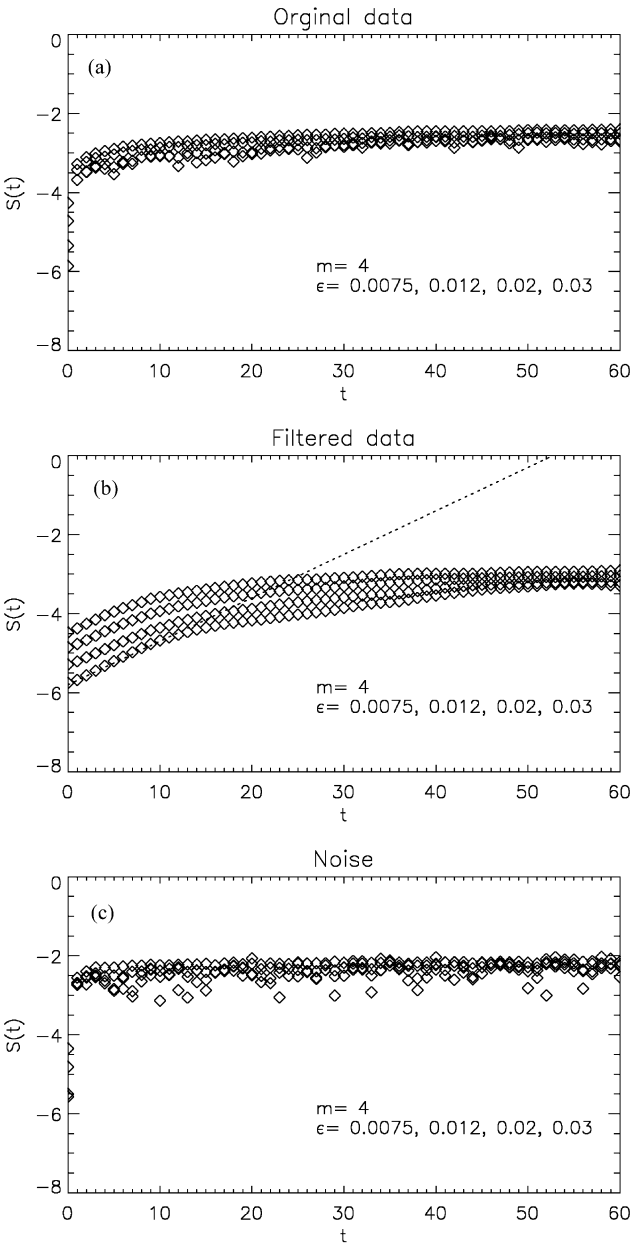

Fig. 4. The function $S(t)$ versus the time step t, for various ε and fixed $m = 4$, obtained for (a) original data after detrending, (b) after nonlinear noise reduction, and (c) noise removed by nonlinear filter. Only in case (b) do we see a linear increase with identical slope (dotted line), which yields the maximal Lyapunov exponent $\lambda_{\max} = 0.10 \pm 0.02$.

in the solar wind flow, and probably in most real complex systems. We have verified the robustness of the main results against the change in both parameters r and m. Thus, we can expect that for sufficiently large m in the scaling region K_2 should converge towards a constant according to Eq. (5). Admittedly, this is merely a certain approximation of the ideal $m \to \infty$ limit in Eq. (3) for $q = 2$.

Finally, the spacings between the parallel lines averaged in the saturation region $8 \leqslant m \leqslant 12$ are taken as $K_2(r)$, see Table 2. These saturated values averaged over ln r for various r in the scaling region, yield the correlation entropy $K_2 = 0.10 \pm 0.06$ (base e), Table 1. A clear saturation of $K_{2,\mathrm{m}}(r)$ in Fig. 3(b) shows that the correlation entropy is *positive* and *finite*, as it should be for a *chaotic* system.

Second, the maximal Lyapunov exponent $\lambda_{\max}$ has been estimated using the algorithm of Kantz (1994). In Fig. 4, the function $S(t) = S(t; m, \varepsilon)$ defined in Eq. (8) is plotted

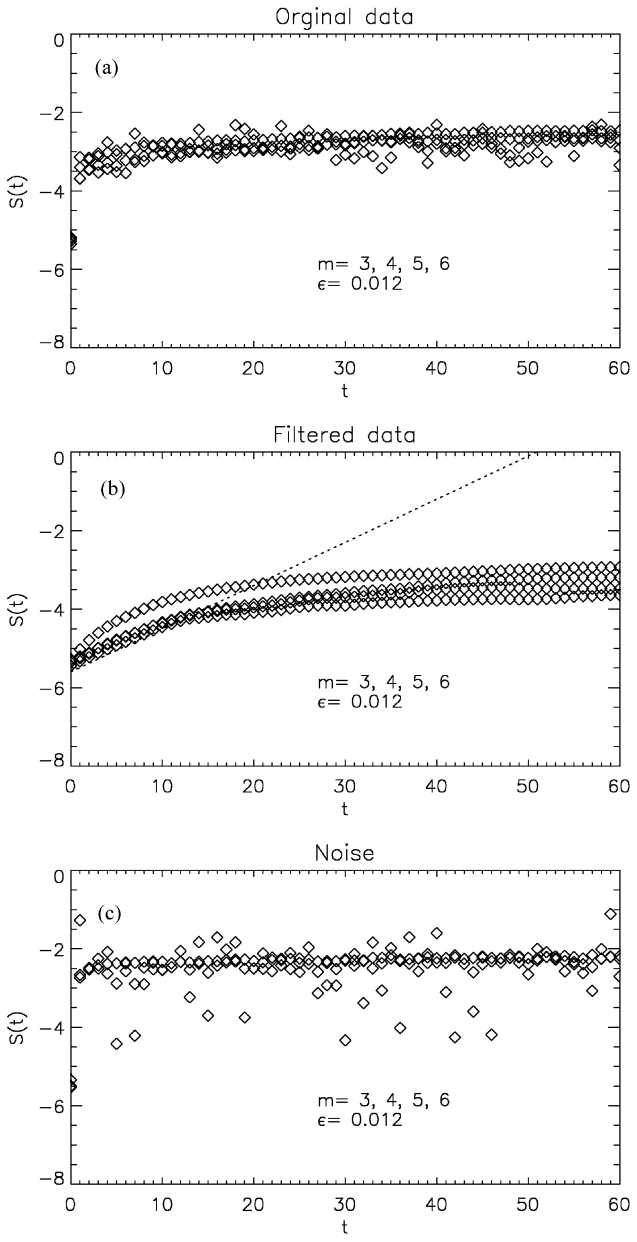

Fig. 5. The function $S(t)$ versus the time step t, for various m and fixed $\varepsilon = 0.012$, obtained for (a) original data after detrending, (b) after nonlinear noise reduction, and (c) noise removed by nonlinear filter. Only in case (b), for $m > 3$, do the curves saturate to the straight dotted line with slope 0.1.

versus the time t for various ε and fixed embedding dimension $m = 4$, larger than the dimension of the attractor (cf. Ding et al., 1993; Takens, 1981). As seen in Fig. 4(a) for the original data, containing about 5% of noise, we cannot observe any linear increase; after few time steps, any initial small distance quickly saturate to a mean absolute distance typical for the attractor. Only after noise reduction, Fig. 4(b), we see a linear increase with the same slope (dotted line), which provides an estimate of the maximal Lyapunov exponent $\lambda_{\max} \approx 0.1$. Outside the scaling region, the function

Table 2
The correlation entropy $K_2(r)$ calculated from the cleaned experimental data

$\ln r$	Average $8 \leqslant m \leqslant 12$
−2.4	0.10 ± 0.03
−2.5	0.10 ± 0.04
−2.6	0.10 ± 0.06
−2.8	0.11 ± 0.07
−2.9	0.11 ± 0.08
Average over $\ln r$	0.10 ± 0.06

Table 3
The maximal Lyapunov exponent $\lambda_{\max}$ calculated from the cleaned experimental data

ε	Average $0 \leqslant t \leqslant 10$
0.03	0.09 ± 0.03
0.02	0.09 ± 0.02
0.012	0.10 ± 0.01
0.0075	0.11 ± 0.01
Average over ε	0.10 ± 0.02

$S(t)$ tends to a small constant, since the distances between vectors cannot grow more than the size of the attractor.

In Fig. 5, we show the same function $S(t)$ versus the time t, but for various embedding dimension m and fixed $\varepsilon = 0.012$. After noise reduction, Fig. 5(b), for embedding dimension $m > 3$ the curves saturate to the straight line with slope $\lambda_{\max} \approx 0.1$. On the contrary, no linear increase can be seen in Fig. 5(a) and (c). In addition, noise gives rise to large fluctuation as the embedding dimension increases.

As well as for the entropy, after nonlinear noise reduction, also for Lyapunov exponent we obtain quite robust results against the change in both parameters m and ε. Using least squares fit for the linear parts of the curves $0 \leqslant t \leqslant 10$, and averaging over ε, we can determine the numerical value of the maximal Lyapunov exponent together with the error of the fit $\lambda_{\max} = 0.10 \pm 0.02$, as shown in Table 3. Naturally, the errors given in Tables 1–3 are obtained assuming their normal distribution over the scaling range and the maximum error in the scaling region is given here. Anyway, we conclude that the largest Lyapunov exponent is *positive* and finite, implying sensitive dependence on initial conditions. Moreover its value is consistent with the correlation entropy $K_2 = 0.10 \pm 0.06$ which should be its lower bound: $K_2 \leqslant \sum \lambda_i$ (positive). The time over which the meaningful prediction of the behaviour of the system is possible is roughly $\sim 1/\lambda_{\max}$, e.g., Ott et al. (1994). Hence the predictability of the system would be limited.

The measures of the attractor obtained have also been subjected to surrogate data tests (Theiler et al., 1992). As is shown in (Macek, 1998, Fig. 8), if the original data are indeed deterministic, analysis of these surrogate data will provide values that are statistically distinct from those

derived for the original data. Again, we have found here that the solar wind data are sensitive to this test. More specifically, if we plot $K_{2,\mathrm{m}}(r)$ for the surrogates random data (with the same scalar distribution as for the original data), we obtain the same behaviour as for the original data for large scale distances r, but no plateau is obtained for small r. This means that for large scales the data cannot be distinguished from random data. In this sense, the determinism becomes visible only below a critical scale of $r \sim e^{-2}$ (Olbrich and Kantz, 1997). Further, contrary to the case of the filtered solar wind data there is no saturation of the function $K_{2,\mathrm{m}}(r)$ for the surrogate data for large m; instead this function increases with m. Similarly, the function $S(t)$ for surrogates does not show any region of linear increase. Distances increase rather diffusively, which corresponds to the fact that the largest Lyapunov exponent is infinite, as it should be for stochastic data (Kantz and Schreiber, 1997).

5. Conclusions

To conclude, small amounts of noise (few percent) obscure scaling properties at small scales, preventing us from any reliable estimation of the Kolmogorov correlation entropy and the largest Lyapunov exponent. The nonlinear Schreiber filter efficiently removes noise (leaving less than one percent) and allows a more realistic estimation of these invariants. The entropy and the largest Lyapunov exponent are plausibly positive locally that would exhibit sensitive dependence on initial conditions. The characteristics of the attractor obtained are significantly different from those of the surrogate data. Hence we suggest that there exists an inertial manifold for the slow solar wind in the inner heliosphere, in which the system is nonlinear and possibly *chaotic*. This means that the observed irregular behaviour of the velocity fluctuations results from intrinsic nonlinear chaotic dynamics rather than from random external forces.

Acknowledgements

This work was supported by the State Scientific Research Committee through Grant No. 2 P03C 001 16. One of us (W.M.M.) thanks H. Rosenbauer and R. Schwenn for introducing the Helios data to him.

References

Albano, A.M., Muench, J., Schwartz, C., Mess, A.I., Rapp, P.E., 1988. Phys. Rev. A 38, 3017–3026.
Badii, R., Broggi, G., Derighetti, B., Ravani, M., Ciliberto, S., Politi, A., Rubio, M.A., 1988. Phys. Rev. Lett. 60, 979–982.
Carbone, V., Veltri, P., Bruno, R., 1995. Phys. Rev. Lett. 75, 3110–3113.
Ding, M., Grebogi, C., Ott, E., Sauer, T., Yorke, J.A., 1993. Phys. Rev. Lett. 70, 3872–3875.
Grassberger, P., Procaccia, I., 1983a. Phys. Rev. A 28, 2591–2593.
Grassberger, P., Procaccia, I., 1983b. Physica D 9, 189–208.
Kantz, H., 1994. Phys. Lett. A 185, 77–87.
Kantz, H., Schreiber, T., 1997. Nonlinear Time Series Analysis. Cambridge University Press, Cambridge.
Kantz, H., Schreiber, T., Hoffmann, I., Buzug, T., Pfister, G., Flepp, L.G., Simonet, J., Badii, R., Brun, E., 1993. Phys. Rev. E 48, 1529–1538.
Kostelich, E.J., Schreiber, T., 1993. Phys. Rev. E 48, 1752–1763.
Kurths, J., Herzel, H., 1987. Physica D 25, 165–172.
Macek, W.M., 1998. Physica D 122, 254–264.
Macek, W.M., 1999. Testing for an attractor in the low-speed solar wind flow. In: Habbal, S.R., Esser, R., Hollweg, J.V., Isenberg, P.A. (Eds.), Solar Wind Nine, Vol. 471. American Institute of Physics, New York, pp. 251–254.
Macek, W.M., Obojska, L., 1996. Fractal analysis of the low-speed solar wind flow. In: Hilgers, A., Guyenne, T.-D. (Eds.), ESA Symposium Proceedings on Environment Modelling for Space-based Applications, SP-392. ESTEC, Noordwijk, pp. 247–252.
Macek, W.M., Obojska, L., 1997. Chaos Solitons Fract. 8, 1601–1607.
Macek, W.M., Obojska, L., 1998. Chaos Solitons Fract. 9, 221–229.
Macek, W.M., Redaelli, S., 2000. Phys. Rev. E 62, 6496–6504.
Olbrich, E., Kantz, H., 1997. Phys. Lett. A 232, 63–69.
Ott, E., 1993. Chaos in Dynamical Systems. Cambridge University Press, Cambridge.
Ott, E., Sauer, T., Yorke, J.A., 1994. Coping with Chaos. Wiley, New York.
Schreiber, T., 1993a. Phys. Rev. E 47, 2401–2404.
Schreiber, T., 1993b. Phys. Rev. E 48, R13–R16.
Schreiber, T., Kantz, H., 1995. Chaos 5, 133–142.
Schuster, H.G., 1989. Deterministic Chaos. VCH, Weinheim, Germany.
Schwenn, R., 1990. Large-scale structure of the interplanetary medium. In: Schwenn, R., Marsch, E. (Eds.), Physics of the Inner Heliosphere, Vol. 20. Springer, Berlin, pp. 99–182.
Takens, F., 1981. Detecting strange attractors in turbulence. In: Rand, D.A., Young, L.S. (Eds.), Dynamical Systems and Turbulence, Lecture Notes in Mathematics, Vol. 898. Springer, Berlin, pp. 366–381.
Theiler, J., 1986. Phys. Rev. A 34, 2427–2432.
Theiler, J., Eubank, S., Longtin, A., Galdrikian, B., Farmer, J.D., 1992. Physica D 58, 77–94.
Wolf, A., Swift, J.B., Swinney, H.L., Vastano, J.A., 1985. Physica D 16, 285–317.